Di-hadron correlations with identified leading hadrons in 200 GeV Au + Au and d + Au collisions at STAR

STAR Collaboration

L. Adamczyk [a], J.K. Adkins [s], G. Agakishiev [q], M.M. Aggarwal [ac], Z. Ahammed [au],
I. Alekseev [o], A. Aparin [q], D. Arkhipkin [c], E.C. Aschenauer [c], G.S. Averichev [q], X. Bai [h],
V. Bairathi [z], A. Banerjee [au], R. Bellwied [aq], A. Bhasin [az], A.K. Bhati [ac], P. Bhattarai [ap],
J. Bielcik [j], J. Bielcikova [k], L.C. Bland [c], I.G. Bordyuzhin [o], J. Bouchet [r], D. Brandenburg [ai],
A.V. Brandin [y], I. Bunzarov [q], J. Butterworth [ai], H. Caines [ay],
M. Calderón de la Barca Sánchez [e], J.M. Campbell [aa], D. Cebra [e], M.C. Cervantes [ao],
I. Chakaberia [c], P. Chaloupka [j], Z. Chang [ao], S. Chattopadhyay [au], X. Chen [u], J.H. Chen [al],
J. Cheng [ar], M. Cherney [i], W. Christie [c], G. Contin [v], H.J. Crawford [d], S. Das [l], L.C. De Silva [i],
R.R. Debbe [c], T.G. Dedovich [q], J. Deng [ak], A.A. Derevschikov [ae], B. di Ruzza [c], L. Didenko [c],
C. Dilks [ad], X. Dong [v], J.L. Drachenberg [at], J.E. Draper [e], C.M. Du [u], L.E. Dunkelberger [f],
J.C. Dunlop [c], L.G. Efimov [q], J. Engelage [d], G. Eppley [ai], R. Esha [f], O. Evdokimov [h], O. Eyser [c],
R. Fatemi [s], S. Fazio [c], P. Federic [k], J. Fedorisin [q], Z. Feng [g], P. Filip [q], Y. Fisyak [c], C.E. Flores [e],
L. Fulek [a], C.A. Gagliardi [ao], D. Garand [af], F. Geurts [ai], A. Gibson [at], M. Girard [av], L. Greiner [v],
D. Grosnick [at], D.S. Gunarathne [an], Y. Guo [aj], S. Gupta [az], A. Gupta [az], W. Guryn [c],
A. Hamad [r], A. Hamed [ao], R. Haque [z], J.W. Harris [ay], L. He [af], S. Heppelmann [c],
S. Heppelmann [ad], A. Hirsch [af], G.W. Hoffmann [ap], D.J. Hofman [h], S. Horvat [ay], T. Huang [c],
B. Huang [h], H.Z. Huang [f], X. Huang [ar], P. Huck [g], T.J. Humanic [aa], G. Igo [f], W.W. Jacobs [n],
H. Jang [t], J. Jia [c], K. Jiang [aj], E.G. Judd [d], S. Kabana [r], D. Kalinkin [o], K. Kang [ar], K. Kauder [aw,*],
H.W. Ke [c], D. Keane [r], A. Kechechyan [q], Z.H. Khan [h], D.P. Kikoła [av], A. Kisiel [av], L. Kochenda [y],
D.D. Koetke [at], L.K. Kosarzewski [av], A.F. Kraishan [an], P. Kravtsov [y], K. Krueger [b], L. Kumar [ac],
M.A.C. Lamont [c], J.M. Landgraf [c], K.D. Landry [f], J. Lauret [c], A. Lebedev [c], R. Lednicky [q],
J.H. Lee [c], X. Li [an], W. Li [al], Z.M. Li [g], Y. Li [ar], C. Li [aj], X. Li [aj], M.A. Lisa [aa], F. Liu [g], T. Ljubicic [c],
W.J. Llope [aw], M. Lomnitz [r], R.S. Longacre [c], X. Luo [g], G.L. Ma [al], Y.G. Ma [al], R. Ma [c], L. Ma [al],
N. Magdy [am], R. Majka [ay], A. Manion [v], S. Margetis [r], C. Markert [ap], H. Masui [v], H.S. Matis [v],
D. McDonald [aq], K. Meehan [e], J.C. Mei [ak], N.G. Minaev [ae], S. Mioduszewski [ao], D. Mishra [z],
B. Mohanty [z], M.M. Mondal [ao], D.A. Morozov [ae], M.K. Mustafa [v], B.K. Nandi [m], Md. Nasim [f],
T.K. Nayak [au], G. Nigmatkulov [y], T. Niida [aw], L.V. Nogach [ae], S.Y. Noh [t], J. Novak [x],
S.B. Nurushev [ae], G. Odyniec [v], A. Ogawa [c], K. Oh [ag], V. Okorokov [y], D. Olvitt Jr. [an],
B.S. Page [c], R. Pak [c], Y.X. Pan [f], Y. Pandit [h], Y. Panebratsev [q], B. Pawlik [ab], H. Pei [g],
C. Perkins [d], A. Peterson [aa], P. Pile [c], J. Pluta [av], K. Poniatowska [av], J. Porter [v], M. Posik [an],
A.M. Poskanzer [v], N.K. Pruthi [ac], J. Putschke [aw], H. Qiu [v], A. Quintero [r], S. Ramachandran [s],
R. Raniwala [ah], S. Raniwala [ah], R.L. Ray [ap], H.G. Ritter [v], J.B. Roberts [ai], O.V. Rogachevskiy [q],
J.L. Romero [e], A. Roy [au], L. Ruan [c], J. Rusnak [k], O. Rusnakova [j], N.R. Sahoo [ao], P.K. Sahu [l],
I. Sakrejda [v], S. Salur [v], J. Sandweiss [ay], A. Sarkar [m], J. Schambach [ap], R.P. Scharenberg [af],

---

* Corresponding author.

A.M. Schmah [v], W.B. Schmidke [c], N. Schmitz [w], J. Seger [i], P. Seyboth [w], N. Shah [al], E. Shahaliev [q], P.V. Shanmuganathan [r], M. Shao [aj], B. Sharma [ac], M.K. Sharma [az], W.Q. Shen [al], S.S. Shi [g], Q.Y. Shou [al], E.P. Sichtermann [v], R. Sikora [a], M. Simko [k], S. Singha [r], M.J. Skoby [n], N. Smirnov [ay], D. Smirnov [c], L. Song [aq], P. Sorensen [c], H.M. Spinka [b], B. Srivastava [af], T.D.S. Stanislaus [at], M. Stepanov [af], M. Strikhanov [y], B. Stringfellow [af], M. Sumbera [k], B. Summa [ad], Y. Sun [aj], Z. Sun [u], X.M. Sun [g], X. Sun [v], B. Surrow [an], D.N. Svirida [o], M.A. Szelezniak [v], A.H. Tang [c], Z. Tang [aj], T. Tarnowsky [x], A. Tawfik [ax], J.H. Thomas [v], A.R. Timmins [aq], D. Tlusty [ai], T. Todoroki [c], M. Tokarev [q], S. Trentalange [f], R.E. Tribble [ao], P. Tribedy [c], S.K. Tripathy [l], O.D. Tsai [f], T. Ullrich [c], D.G. Underwood [b], I. Upsal [aa], G. Van Buren [c], G. van Nieuwenhuizen [c], M. Vandenbroucke [an], R. Varma [m], A.N. Vasiliev [ae], R. Vertesi [k], F. Videbæk [c], Y.P. Viyogi [au], S. Vokal [q], S.A. Voloshin [aw], A. Vossen [n], J.S. Wang [u], F. Wang [af], H. Wang [c], G. Wang [f], Y. Wang [ar], Y. Wang [g], G. Webb [c], J.C. Webb [c], L. Wen [f], G.D. Westfall [x], H. Wieman [v], S.W. Wissink [n], R. Witt [as], Y.F. Wu [g], Wu [r], Z.G. Xiao [ar], W. Xie [af], K. Xin [ai], H. Xu [u], Z. Xu [c], Q.H. Xu [ak], Y.F. Xu [al], N. Xu [v], S. Yang [aj], Y. Yang [c], Q. Yang [aj], Y. Yang [u], C. Yang [aj], Y. Yang [g], Z. Ye [h], Z. Ye [h], P. Yepes [ai], L. Yi [ay], K. Yip [c], I.-K. Yoo [ag], N. Yu [g], H. Zbroszczyk [av], W. Zha [aj], Y. Zhang [aj], Z. Zhang [al], J.B. Zhang [g], J. Zhang [ak], X.P. Zhang [ar], S. Zhang [al], J. Zhang [u], J. Zhao [g], C. Zhong [al], L. Zhou [aj], X. Zhu [ar], Y. Zoulkarneeva [q]

[a] *AGH University of Science and Technology, Cracow 30-059, Poland*
[b] *Argonne National Laboratory, Argonne, IL 60439, USA*
[c] *Brookhaven National Laboratory, Upton, NY 11973, USA*
[d] *University of California, Berkeley, CA 94720, USA*
[e] *University of California, Davis, CA 95616, USA*
[f] *University of California, Los Angeles, CA 90095, USA*
[g] *Central China Normal University (HZNU), Wuhan 430079, China*
[h] *University of Illinois at Chicago, Chicago, IL 60607, USA*
[i] *Creighton University, Omaha, NE 68178, USA*
[j] *Czech Technical University in Prague, FNSPE, Prague, 115 19, Czech Republic*
[k] *Nuclear Physics Institute AS CR, 250 68 Řež/Prague, Czech Republic*
[l] *Institute of Physics, Bhubaneswar 751005, India*
[m] *Indian Institute of Technology, Mumbai 400076, India*
[n] *Indiana University, Bloomington, IN 47408, USA*
[o] *Alikhanov Institute for Theoretical and Experimental Physics, Moscow 117218, Russia*
[p] *Univenrsity of Jammu, Jammu 180001, India*
[q] *Joint Institute for Nuclear Research, Dubna, 141 980, Russia*
[r] *Kent State University, Kent, OH 44242, USA*
[s] *University of Kentucky, Lexington, KY, 40506-0055, USA*
[t] *Korea Institute of Science and Technology Information, Daejeon 305-701, Republic of Korea*
[u] *Institute of Modern Physics, Lanzhou 730000, China*
[v] *Lawrence Berkeley National Laboratory, Berkeley, CA 94720, USA*
[w] *Max-Planck-Institut fur Physik, Munich 80805, Germany*
[x] *Michigan State University, East Lansing, MI 48824, USA*
[y] *Moscow Engineering Physics Institute, Moscow 115409, Russia*
[z] *National Institute of Science Education and Research, Bhubaneswar 751005, India*
[aa] *Ohio State University, Columbus, OH 43210, USA*
[ab] *Institute of Nuclear Physics PAN, Cracow 31-342, Poland*
[ac] *Panjab University, Chandigarh 160014, India*
[ad] *Pennsylvania State University, University Park, PA 16802, USA*
[ae] *Institute of High Energy Physics, Protvino 142281, Russia*
[af] *Purdue University, West Lafayette, IN 47907, USA*
[ag] *Pusan National University, Pusan 609735, Republic of Korea*
[ah] *University of Rajasthan, Jaipur 302004, India*
[ai] *Rice University, Houston, TX 77251, USA*
[aj] *University of Science and Technology of China, Hefei 230026, China*
[ak] *Shandong University, Jinan, Shandong 250100, China*
[al] *Shanghai Institute of Applied Physics, Shanghai 201800, China*
[am] *State University Of New York, Stony Brook, NY 11794, USA*
[an] *Temple University, Philadelphia, PA 19122, USA*
[ao] *Texas A&M University, College Station, TX 77843, USA*
[ap] *University of Texas, Austin, TX 78712, USA*
[aq] *University of Houston, Houston, TX 77204, USA*
[ar] *Tsinghua University, Beijing 100084, China*
[as] *United States Naval Academy, Annapolis, MD, 21402, USA*
[at] *Valparaiso University, Valparaiso, IN 46383, USA*
[au] *Variable Energy Cyclotron Centre, Kolkata 700064, India*
[av] *Warsaw University of Technology, Warsaw 00-661, Poland*
[aw] *Wayne State University, Detroit, MI 48201, USA*
[ax] *World Laboratory for Cosmology and Particle Physics (WLCAPP), Cairo 11571, Egypt*

[ay] *Yale University, New Haven, CT 06520, USA*
[az] *University of Jammu, Jammu 180001, India*

ARTICLE INFO

ABSTRACT

The STAR Collaboration presents for the first time two-dimensional di-hadron correlations with identified leading hadrons in 200 GeV central Au + Au and minimum-bias d + Au collisions to explore hadronization mechanisms in the quark gluon plasma. The enhancement of the jet-like yield for leading pions in Au + Au data with respect to the d + Au reference and the absence of such an enhancement for leading non-pions (protons and kaons) are discussed within the context of a quark recombination scenario. The correlated yield at large angles, specifically in the *ridge region*, is found to be significantly higher for leading non-pions than pions. The consistencies of the constituent quark scaling, azimuthal harmonic model and a mini-jet modification model description of the data are tested, providing further constraints on hadronization.

Experimental data from heavy-ion collisions at ultra-relativistic energies achieved at the Relativistic Heavy Ion Collider (RHIC), and more recently at the Large Hadron Collider (LHC), are conventionally interpreted in terms of a unique form of matter, the strongly-interacting Quark Gluon Plasma (sQGP). It is estimated that temperatures reached in those collisions [1,2] are well above the critical values predicted by lattice quantum chromodynamics calculations for the phase transition between hadronic and deconfined (partonic) matter [3]. The RHIC experiments concluded that the formed medium displays the properties of a nearly perfect liquid [4]. A distinct feature of the sQGP is jet quenching, which describes the large energy loss of "hard" (high transverse momentum, p_T) probes observed for example in measurements of inclusive hadron distributions [5].

Jet quenching is also evident in modifications of back-to-back di-hadron correlations with a leading (high-p_T) "trigger" hadron in Au + Au collisions in comparison to p + p and d + Au data [6–10]. One of the striking features found in di-hadron correlations from heavy-ion collisions is the emergence of a long-range plateau in relative pseudorapidity ($\Delta\eta$) on the near-side of a trigger hadron (small relative azimuth $\Delta\phi$), referred to as the "ridge" [6–8]. The majority of recent theoretical descriptions of this phenomenon invoke a transport of initial-state to final-state anisotropy via hydrodynamic expansion, thus connecting measured observables to transport coefficients and properties of the medium [11–13]. Most of the proposed alternative explanations also require hydrodynamic evolution of the medium to reproduce the ridge [14]. The latest observations of ridge-like correlations in high-multiplicity p + p and p + Pb collisions at the LHC provide new tests of theoretical explanations of the ridge [15,16].

Another anomaly, the enhancement of the relative baryon-to-meson production, was discovered at RHIC in the intermediate-p_T range between 2 and 5 GeV/c, where the ridge happens to be most prominent [17–20]. The ratio of proton to pion yields in central Au + Au collisions exceeds by more than a factor of two that in d + Au and p + p events. Similar baryon enhancements were reported in the strange-hadron sector [21,22]. In the same kinematic region, baryons and mesons exhibit different trends in azimuthal anisotropy, which at RHIC appear to scale with the number of constituent quarks [23]. Recombination models, which incorporate the coalescence of two or three constituent quarks as a formation mechanism for mesons and baryons, are able to reproduce the observed enhancements in inclusive measurements [24]. Description of hadronization processes remains challenging for theoretical calculations (see for example the unexpected measurements reported in Ref. [25]); we expect these new measurements will facilitate further developments in this area.

In this Letter, we use angular correlations of intermediate-p_T particles with identified leading hadrons to further explore possible hadronization mechanisms in the quark gluon plasma, including changes to parton fragmentation patterns, dilution effects (reduction in per-trigger yields) due to recombination contributions, and quark number scaling behavior in correlations at large relative angles.

Two-dimensional di-hadron correlations in $\Delta\phi$ and $\Delta\eta$, with statistically separated pion and non-pion triggers, are studied for the 0–10% most-central Au + Au and minimum-bias d + Au collisions at the center-of-mass energy per nucleon pair $\sqrt{s_{NN}} = 200$ GeV. No charge separation is considered; in this paper, the terms pion, proton, and kaon will be used to refer to the sum of particles and their respective anti-particles. We separately study the short-range (jet-like peak) and long-range (ridge) correlations in central Au + Au data, comparing to reference measurements performed in d + Au collisions. Details of the short-range correlations can shed light on the interplay between parton fragmentation, energy loss, and recombination processes in the quark gluon plasma. The long-range correlations are studied with two approaches: (1) Fourier decomposition where we extract the azimuthal harmonic amplitudes which in some approaches are interpreted as hydrodynamic "flows" [12], and (2) a mini-jet (defined in [26]) modification model [26,27].

The analysis was conducted using 1.52×10^8 central-triggered Au + Au events at $\sqrt{s_{NN}} = 200$ GeV from STAR's 2010 data run, and 4.6×10^7 events from the 2008 minimum-bias 200 GeV d + Au data set. Particle densities as well as Glauber Monte Carlo results for these centrality selections can be found in Ref. [28]. The STAR Time Projection Chamber (TPC) [29] was used for tracking, momentum reconstruction and particle identification. Contamination by tracks from another collision ("pileup"), which can distort the shape of di-hadron correlations [26], was removed by rejecting events with an abnormally large (over three standard deviations above the average) number of tracks not originating from the primary vertex.

Trigger particles are defined as the highest-p_T charged hadron in a given event with p_T^{trig} between 4 and 5 GeV/c; charged hadrons between 1.5 and 4 GeV/c are associated with each trigger particle. This kinematic range focuses on a particularly interesting region where trigger particle production is thought to be dominated by fragmentation, at least in pp and d + Au collisions. For the same range in Au + Au events, the baryon-to-meson enhancement is large, suggesting significant recombination contributions [30]. Since the medium induced jet quenching affects the correlations in essentially an opposite way from thermal parton recombination contributions, comparing the correlations for proton and pion triggers provides an additional handle for separating these effects.
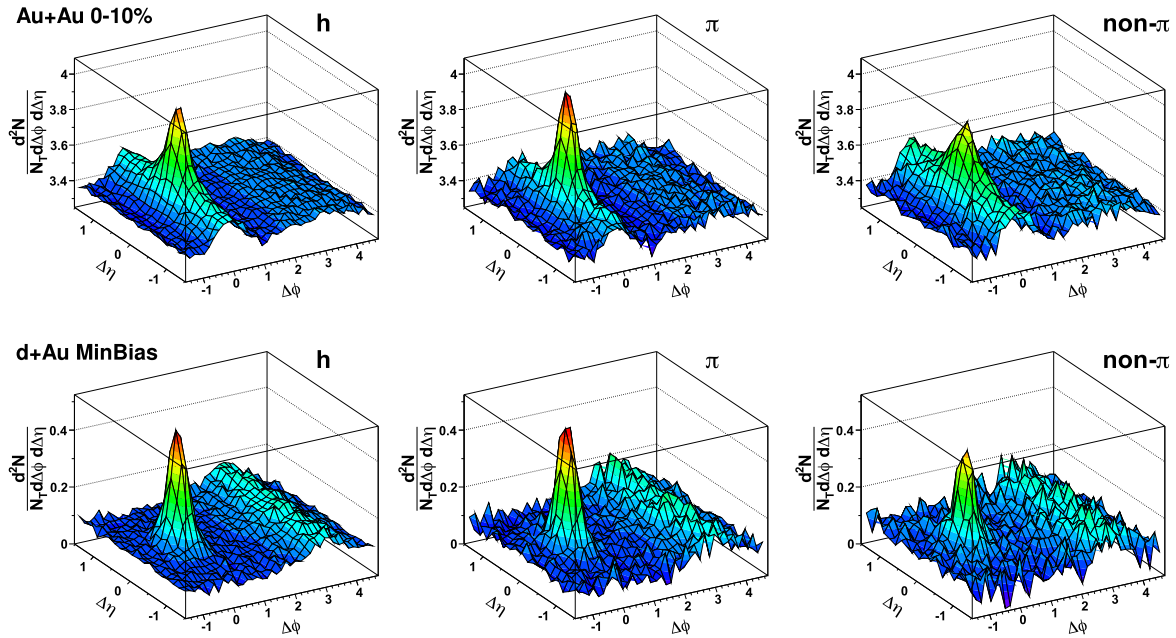
Fig. 1. (Color online.) Two-dimensional $\Delta\phi$ vs. $\Delta\eta$ correlation functions for charged hadron (left), pion (middle), and non-pion (right) triggers from 0–10% most-central Au + Au (top row) and minimum-bias d + Au (bottom row) data at 200 GeV. All trigger and associated charged hadrons are selected in the respective p_T ranges $4 < p_T^{\rm trig} < 5$ GeV/c and $1.5 < p_T^{\rm assoc} < 4$ GeV/c.

Also, the ridge and away-side modifications in this p_T range are significant, and elliptic flow, and its p_T dependence, are minimal, thus facilitating the present tests of constituent quark number scaling. All trigger particles are required to have at least 30 TPC points per track (for optimal identification), otherwise, standard quality cuts and corrections are applied as described in Ref. [8]. After quality cuts, 3.5×10^6 Au + Au and 1×10^5 d + Au events with a trigger particle were used for the analysis. The statistical hadron identification procedure relies on the measured ionization energy loss (dE/dx) in the TPC gas. The dE/dx calibration was carried out individually for five pseudorapidity and two trigger p_T bins. Details of the particle identification (PID) technique are identical to those in Refs. [17,28,31].

We construct a two-dimensional correlation with each trigger and all associated hadrons in an event, following the procedure outlined in Ref. [8]. Pion identification is straightforward: selecting triggers with dE/dx above the central (expected) pion value provides a sample with 98% pion purity and, by construction, 50% selection efficiency. The "pure-pion" correlation is constructed with those triggers. The remaining triggers are comprised of all protons, about 97% of all kaons, and the remaining 50% of pions.

We remove the pion contribution from the correlation with those remaining triggers by direct subtraction of the pure-pion-triggered correlation. The resulting "non-pion" correlation is then associated with a mixture of proton and kaon triggers (about three protons for every two kaons [32]). Separating kaons from protons is complicated by the small dE/dx difference between the two and was not attempted in this Letter. The systematic uncertainty due to the pion subtraction procedure is included in the PID uncertainty. The evaluation procedure is similar to previous identified particle analyses with the STAR Time Projection Chamber, where sensitivities of the final observables to systematic variations in the dE/dx cut parameters were determined. The feed-down contribution from weak decay daughters to the trigger particles cannot be disentangled directly. Due to decay kinematics, the dominant feed-down contribution originates from $\Lambda \rightarrow p\pi$ and is estimated to constitute about 5% of the non-pion triggers. Resonance contributions are greatly suppressed at high p_T and shown to give only

minor contributions to correlation structures [26]. All raw correlation functions are corrected for detector inefficiency derived from Monte Carlo tracks embedded into real data as in Refs. [8,9,28]. Pair-acceptance effects are corrected using the mixed-event technique as in Ref. [9]. The resulting correlations are shown in Fig. 1, with visible differences between the two trigger types in both jet-like peak and large $\Delta\eta$ region in Au + Au. A significantly larger ridge amplitude is seen for non-pion triggers, while the jet-like peak is more pronounced for the pion triggers. By comparison, the correlations in d + Au show no discernible ridge on the near-side, while differences between trigger types in the jet-like region are qualitatively similar to Au + Au, suggesting that these may be partly due to kinematic effects. In the following, we analyze these modifications individually.

Initially, we study the small-angle jet-like correlated signals. Assuming that all background contributions are $\Delta\eta$-independent, as shown in Refs. [8,33], we subtract those contributions averaged over large $|\Delta\eta| = 0.9$–1.5 from the full correlations, resulting in "pure-cone" distributions. This procedure is supported by the two-dimensional fits to the data described below. We then calculate the fiducial jet-like yield in $|\Delta\eta| < 0.78$, $|\Delta\phi| < \pi/4$ as in Ref. [7]. To isolate medium effects from initial-state nuclear effects, the Au + Au results are then compared to the correlation function constructed in an identical way for d + Au data (see Fig. 2). We report significant differences in the jet-like yield per trigger between the two systems for pion triggers. At the same time, correlations with non-pion triggers show, within uncertainties, similar yields for the two systems. For quantitative comparisons, the integrated yields are presented in Table 1. The yield extrapolation outside the fiducial range is performed using cone-shape modeling described below. The systematic errors are dominated by the tracking efficiency uncertainty (5%); other sources include uncertainties from p_T resolution (3%), PID uncertainty (2–3%), background level determination (2% for Au + Au, 2–5% for d + Au; found by varying the range for the $\Delta\eta$-independent ridge structure between $|\Delta\eta| = 0.8$–1.4 and $|\Delta\eta| = 1.0$–1.6), track splitting/merging correction (1%), and pair acceptance (<1%). The effect of feed-down protons on the jet-like yield is estimated to be less than 1%.
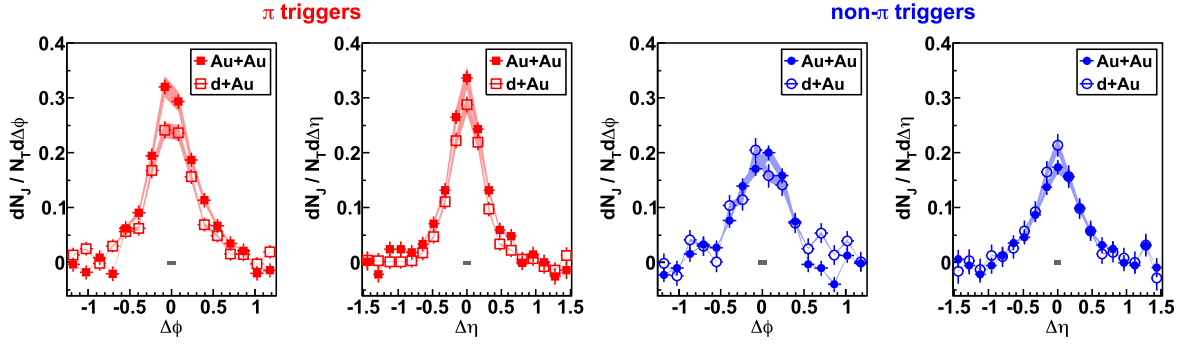
π triggers   **non-π triggers**

Fig. 2. (Color online.) The $\Delta\phi$ and $\Delta\eta$ projections of the pure-cone correlations for $|\Delta\eta| < 0.78$ and $|\Delta\phi| < \pi/4$, respectively, for pion triggers (left two panels) and non-pion triggers (right two panels). Filled symbols show data from the 0–10% most-central Au + Au collisions at 200 GeV; open symbols show data from minimum-bias d + Au data at the same energy. Shaded boxes centered at zero show the uncertainty in background level determination; colored bands show the remaining systematic uncertainties.

Table 1

Fiducial ($[|\Delta\eta| < 0.78] \times [|\Delta\phi| < \pi/4]$) and extrapolated pure-cone yields for pion, non-pion and charged hadron (unidentified) triggers (see text), and the associated yield ratios.

Trigger	Au + Au 0–10%				d + Au MinBias			
	Fid.	Ext.	Stat.	Sys.	Fid.	Ext.	Stat.	Sys.
π	0.211	0.214	3%	7%	0.171	0.171	4%	6%
non-π	0.136	0.142	5%	6%	0.142	0.148	7%	8%
All	0.176	0.180	2%	5%	0.161	0.168	2%	5%
$\frac{Y(\text{non-}\pi)}{Y(\pi)}$	0.643	0.662	6%	5%	0.835	0.866	8%	8%

The jet-like yield in the p_T range 1.5-4 GeV/c associated with pion triggers in central Au + Au collisions is enhanced by 24 ± 6(stat.) ± 11(sys.)% with respect to the reference measurement in d + Au. The yields for non-pion triggers are found to be similar between the two systems. A previous work found similar trends in near-side associated yields [34]; however, in that one-dimensional analysis, no separation between jet-like peak and ridge contributions was possible. We find that the jet-like yield for unidentified charged hadron triggers is also enhanced, consistent with our identified trigger results. The enhancement of the jet-like yield of soft hadrons associated with pion triggers could be caused by the jet-quenching effect and/or medium-induced modification of fragmentation functions, and is qualitatively consistent with other observations from non-identified correlations [35] and direct jet measurements [36–38] for low p_T hadrons. It is expected that a larger fraction of non-pion triggers are produced from gluon-jets rather than quark-jets compared to pion triggers [32,39,40]. A predicted higher energy loss for in-medium gluons should then result in even larger jet-like yields for non-pion triggers [41]. On the other hand, particle production from recombination should produce smaller yields than particle production from hard processes (fragmentation) [30], thus diluting (reducing) per-trigger associated yields. This dilution effect would be stronger for baryons, as more intermediate-p_T baryons than mesons are expected to be formed through such a mechanism. The associated yields for non-pion triggers combine both of these competing effects. Thus the observed reduction could be due to a larger recombination effect relative to that from the increased energy loss expected for non-pion leading particles.

The ratio of associated yields for non-pion and pion leading hadrons is shown in Table 1 for Au + Au and d + Au systems. In these ratios, dominant contributions to systematic uncertainties from the tracking efficiency estimate cancel out. The double-ratio constructed from these two results quantifies the relative decrease in associated jet-like yields for non-pion triggers with respect to leading pion results in Au + Au compared to d + Au. This double-ratio, 0.76 ± 0.08(stat.) ± 0.07(sys.), can measure the net effect

of the competition between higher energy loss/higher associated yields at lower p_T for gluon jets versus reduced yields due to recombination in central Au+Au collisions. Currently, no quantitative predictions for either of these two mechanisms are available for direct comparison with data.

Outside of the jet-like cone region, we find no $\Delta\eta$-dependence in the correlated yields within our fiducial range. To characterize the long-range contributions in Au + Au, we perform two-dimensional fits to the full correlation with two different models. One model attributes the ridge to modified fragmentation of produced mini-jets, and the other explains it in terms of higher-order hydrodynamic flows. In both models, the near-side jet-like peak is mathematically characterized by a two-dimensional generalized Gaussian $e^{-(|\Delta\phi|/\alpha_\phi)^{\beta_\phi}} e^{-(|\Delta\eta|/\alpha_\eta)^{\beta_\eta}}$. The resulting fit parameters for the jet cone are found to be identical between the two models and were used for extrapolation of the jet-like cone yields presented in Table 1.

The $\Delta\phi$ projections of the pseudorapidity-independent parts of the two-dimensional correlations (after subtracting the jet-like peak), are shown in Fig. 3, panel (a), together with both fit functions discussed below. Also shown is the corresponding projection for d + Au data, shifted by an arbitrary offset. We performed the Fourier analysis on this data as well; without an appreciable near-side ridge, the above mini-jet model is not applicable here.

In the flow-based approach, based on a hydrodynamic expansion of an anisotropic medium, all $\Delta\eta$-independent parts of the correlations are described via Fourier expansion: $A(1 + \sum_{n=1}^{N} 2V_n \cos n\Delta\phi)$, where A describes the magnitude of the uncorrelated background, V_2 is conventionally associated with "elliptic flow", and V_3 with "triangular flow". In this work, the first five terms ($N = 5$) exhaust all features of the correlation to the level of statistical uncertainty, and V_n represents the combined trigger and associated hadron anisotropy parameters. We note that in this approach, the fragmentation contributions to the away-side correlations in central Au + Au data are expected to be strongly suppressed relative to flow effects by quenching, and they are therefore neglected [11,12]. In the d + Au data, on the contrary, the away-side jet contributions dominate and no appreciable near-side correlated yield at large $\Delta\eta$ is present.

The Fourier fit results are shown in Fig. 3 (b). In Au + Au, the second harmonic is dominant in all long-range correlations for the central data, followed by the triangular (V_3) term. Higher-order harmonic amplitudes rapidly decrease. All harmonic amplitudes for non-pion triggers are found to be larger than those for pion triggers, which is qualitatively consistent with recombination expectations.

The corresponding Fourier harmonics in d + Au are found to be consistent with expectations for a decomposition of a Gaussian
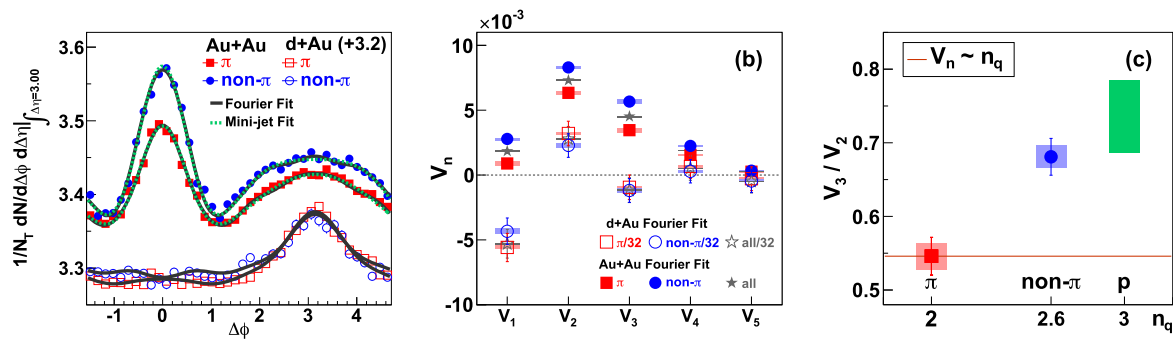
Fig. 3. (Color online.) (a) $\Delta\phi$ projections over $|\Delta\eta| < 1.5$ in 0–10% Au + Au and minimum-bias d + Au data at 200 GeV after subtracting the jet-like fit components. Overlapping dashed and dotted lines illustrate the results of the two-dimensional fits for the flow- and mini-jet based models, respectively. Only statistical errors are shown. (b) Solid symbols show extracted Fourier coefficients from fitting in $\left(\frac{\pi}{2} < \Delta\phi < \frac{3\pi}{2}\right) \times (|\Delta\eta| < 1.5)$ (1.52 for d + Au), for pion, non-pion, and charged hadron triggers in the flow-based model. Open symbols show d + Au data, scaled by the ratio of background levels. (c) V_3/V_2 ratio for pion and non-pion triggers in Au + Au, and the extrapolated value for "pure protons", as described in the text. In all panels, statistical errors are shown as lines (smaller than symbol size for some points), and systematic uncertainties as colored boxes in panels (b) and (c).

peak at π, i.e. rapidly falling and with alternating signs. For $n = 3$, the harmonics are already consistent with zero within errors, confirming that the Fourier and mini-jet approaches are indistinguishable in this case.

In central Au + Au collisions at RHIC, elliptic flow parameters of identified hadrons have been shown to scale with the number of constituent quarks n_q, suggesting collective behavior at the partonic level [23]. The estimated baryon/meson ratio for V_2 in this analysis is also consistent with 3/2, see below. We note that in our trigger p_T range, azimuthal anisotropy is approximately independent of p_T [42], eliminating the need to address quark momentum dependence. To test whether this scaling extends to the triangular term, we examine the V_3/V_2 ratios. This test assumes that the measured Fourier coefficients factorize into $V_n = \langle v_n^{\text{trig}} \rangle \langle v_n^{\text{assc}} \rangle$, where v_n^{trig} and v_n^{assc} measure azimuthal anisotropies of trigger and associated hadrons, respectively [12]. The factorization has been demonstrated experimentally for V_2 in [43]. The extracted V_2 coefficients are found consistent with the product of previously measured identified and unidentified v_2 values. Since the selection of associated particles is identical for all correlations in this analysis, the anisotropy contributions from associated hadrons should cancel in the ratios of V_n coefficients. Fig. 3 (c) shows V_3/V_2 ratios extracted from long-range correlations versus average n_q per particle for pion and non-pion triggers. The systematic uncertainty, determined by varying the fitting range and the dE/dx cut position for pion/non-pion separation, was found to be similar to, or smaller than, the statistical uncertainty. We find that the ratio of triangular and elliptic flow is $0.546 \pm 0.025(\text{stat.}) \pm 0.018(\text{sys.})$ for pion triggers and $0.681 \pm 0.025(\text{stat.}) \pm 0.015(\text{sys.})$ for non-pions. If the measured final-state azimuthal anisotropies are indeed of collective partonic origin which transform into final-state hadronic observables through the coalescence/recombination of constituent quarks, then we would expect the same dependence of all v_n^{trig} on constituent quark number. Even with the significant meson contribution to non-pion triggers, the ratios give a strong indication of a breaking of the simple n_q scaling behavior between the second and third Fourier harmonics. Assuming that kaons, as mesons, adhere to the pion scaling trend, and using the known p/π ratio reported in Ref. [32], we construct an estimate of the V_3/V_2 ratio for pure protons in Fig. 3 (c). The systematic uncertainty in the estimated "pure-proton" V_3/V_2 value of $0.736 \pm 0.038(\text{stat.}) \pm 0.032(\text{sys.})$ includes an additional 1% uncertainty from PID. Feed-down protons from Λ closely preserve the original parent direction, and we expect no measurable effect on the $\Delta\eta$-independent terms, as Λ and protons have very similar azimuthal anisotropy in our kinematic range.

Table 2
First and second harmonic extracted using the mini-jet model in 0–10% most central Au + Au data at 200 GeV. Note that the amplitudes are multiplied by 100.

Trigger	$100(V_1 \pm \text{stat.} \pm \text{sys.})$	$100(V_2 \pm \text{stat.} \pm \text{sys.})$
π	$-0.86 \pm 0.09 \pm 0.07$	$-0.017 \pm 0.045 \pm 0.034$
non-π	$-1.53 \pm 0.13 \pm 0.08$	$-0.343 \pm 0.059 \pm 0.041$
all	$-1.19 \pm 0.05 \pm 0.01$	$-0.173 \pm 0.025 \pm 0.004$

The observed violation of constituent quark number scaling for V_3, based on the "pure proton" extrapolated value for V_3, $V_3(\text{baryon})/V_3(\text{meson}) = 2.03 \pm 0.12(\text{stat.}) \pm 0.20(\text{sys.})$ compared to $V_2(\text{baryon})/V_2(\text{meson}) = 1.50 \pm 0.06(\text{stat.}) \pm 0.07(\text{sys.})$, is intriguing because recombination/coalescence models are the only ones presently capable of describing constituent quark scaling behavior among the V_2 parameters for many identified hadrons.

The difference between the V_3 and V_2 scaling behavior demonstrated in Fig. 3(c) therefore suggests the need for other contributions to long-range correlations to explain the data. We note that deviations from n_q scaling of elliptic flow have been observed at the LHC [44], and at RHIC for non-central collisions [45]. The v_n scaling proposed in Ref. [46] better describes our measured V_3/V_2 ratios, but still under-predicts the enhancement for non-pion triggers.

In the mini-jet model, in which the major component is in-medium modification of fragmentation, only the first two terms ($N = 2$) of the Fourier expansion are kept and the near-side ridge in this analysis is modeled by a one-dimensional Gaussian, resulting in $A(1 + 2V_1 \cos\Delta\phi + 2V_2 \cos 2\Delta\phi) + B e^{-\Delta\phi^2/2\sigma^2}$. Here A is the uncorrelated yield, B is the ridge amplitude, and σ is the ridge width parameter. The dipole V_1 is designated to describe the away-side jet and/or momentum conservation effects, and V_2 describes a non-jet quadrupole (potentially of flow origin). The addition of the 1D near-side Gaussian, which differs from the original model elements in Ref. [26], was necessary to reproduce the data, as noted in Ref. [27]. The mini-jet model fit describes the measured Au + Au correlations for all three trigger types as well as the flow-based approach (Fig. 3(a)), yielding identical uniformly distributed residuals and χ^2 values. The extracted harmonic amplitudes are shown in Table. 2. As the away-side structure is for the most part described by the dipole term, the magnitude of the V_1 amplitude is found to be significantly larger for leading non-pions than for pions. For back-to-back jets, this V_1 increase is supposed to balance the near-side (leading) jet contributions, which would have to consist of both the jet-like peak and the ridge because the jet-like peak alone decreases for non-pion trigger particles. Understanding the behavior of the V_2 term in the mini-jet model fits is challeng-

ing: the V_2 amplitude, while consistent with zero for pion triggers, is significantly negative for non-pion triggers. This negative value for V_2, which is conventionally associated with elliptic flow, is not expected from any known source and calls into question the applicability of the assumed parameterization for the centrality and p_T range studied here, the validity of the "mini-jets + quadrupole only" physics scenario, or both.

In summary, a statistical separation of pion and non-pion triggers was performed to study the systematic behavior of di-hadron correlations from central Au + Au and minimum-bias d + Au collisions at 200 GeV with the STAR experiment. The correlations, decomposed into short- and long-range parts in $\Delta\eta$, are analyzed for different identified trigger types to test the consistency of two models in order to improve our understanding of hadronization mechanisms in the quark gluon plasma. We find significant enhancement of intermediate-p_T charged-hadron jet-like yields associated with pion triggers relative to a d + Au reference measurement. The enhancement is qualitatively consistent with observed modifications of jet fragmentation functions measured at the LHC, suggesting it results from the energy loss process. For the non-pion trigger sample, a larger contribution from gluon fragmentation is expected compared to pion triggers [32,39,40]. Due to the color-charge factor, a larger energy loss for gluons is expected relative to that of quarks. No enhancement is observed for non-pion triggers in contrast to pQCD-based expectations for color charge dependence of energy loss. This lack of enhancement may indicate a competition between parton–medium interaction effects and dilution of jet triggers by quark recombination contributions.

No statistically significant ridge is found associated with either trigger type in minimum bias d + Au data. In Au + Au data, we find a significantly larger ridge-like yield and away-side correlation strength for non-pion than for pion triggers. Two fitting models which are mathematically similar but which are based on distinct physical assumptions were applied to the Au + Au data. Both models, while describing the correlations well, attain parameter values which are problematic within the assumed physical scenarios. In the flow model, the observed differences of V_3/V_2 ratios imply that the explanation of the ridge and away-side modifications as resulting only from hydrodynamic flow of a partonic medium with constituent quark recombination at hadronization is incomplete. On the other hand, the negative V_2 result for the mini-jet based model for leading non-pions indicates that for the data reported here, either the assumed scenario or the mathematical parameterization for jets and dijets is inadequate, or both. These results may have significant implications for understanding the origin of the ridge and hadronization in the QGP.

Acknowledgements

References

[1] A. Adare, et al., PHENIX Collaboration, Phys. Rev. Lett. 104 (2010) 132301.
[2] M. Wilde, ALICE Collaboration, Nucl. Phys. A 904–905 (2013) 573c.
[3] F. Karsch, Nucl. Phys. A 698 (2002) 199.
[4] J. Adams, et al., STAR Collaboration, Nucl. Phys. A 757 (2005) 102;
K. Adcox, et al., PHENIX Collaboration, Nucl. Phys. A 757 (2005) 184;
B. Back, et al., PHOBOS Collaboration, Nucl. Phys. A 757 (2005) 28;
I. Arsene, et al., BRAHMS Collaboration, Nucl. Phys. A 757 (2005) 1.
[5] J. Adams, et al., STAR Collaboration, Phys. Rev. Lett. 91 (2003) 172302;
S.S. Adler, et al., PHENIX Collaboration, Phys. Rev. Lett. 91 (2003) 072303.
[6] J. Adams, et al., STAR Collaboration, Phys. Rev. Lett. 95 (2005) 152301.
[7] B.I. Abelev, et al., STAR Collaboration, Phys. Rev. C 80 (2009) 064912.
[8] G. Agakishiev, et al., STAR Collaboration, Phys. Rev. C 85 (2012) 014903.
[9] M. Aggarwal, et al., STAR Collaboration, Phys. Rev. C 82 (2010) 024912.
[10] J. Adams, et al., STAR Collaboration, Phys. Rev. Lett. 91 (2003) 072304;
A. Adare, et al., PHENIX Collaboration, Phys. Rev. Lett. 98 (2007) 232302;
A. Adare, et al., PHENIX Collaboration, Phys. Rev. C 78 (2008) 014901;
H. Agakishiev, et al., STAR Collaboration, Phys. Rev. C 83 (2011) 061901;
B.I. Abelev, et al., STAR Collaboration, Phys. Rev. Lett. 105 (2010) 022301.
[11] B. Alver, G. Roland, Phys. Rev. C 81 (2010) 054905;
B. Alver, G. Roland, Phys. Rev. C 82 (2010) 039903 (Erratum).
[12] M. Luzum, Phys. Lett. B 696 (2011) 499.
[13] C. Gale, S. Jeon, B. Schenke, Int. J. Mod. Phys. A 28 (2013) 1340011.
[14] C.-Y. Wong, Phys. Rev. C 84 (2011) 024901;
R.C. Hwa, L. Zhu, arXiv:1101.1334;
C. Andrés, A. Moscoso, C. Pajares, arXiv:1405.3632;
G. Moschelli, S. Gavin, Nucl. Phys. A 836 (2010) 43;
H. Petersen, V. Bhattacharya, S.A. Bass, C. Greiner, Phys. Rev. C 84 (2011) 054908;
X. Zhang, J. Liao, arXiv:1311.5463;
A. Dumitru, K. Dusling, F. Gelis, J. Jalilian-Marian, T. Lappi, R. Venugopalan, Phys. Lett. B 697 (2011) 21.
[15] V. Khachatryan, et al., CMS Collaboration, J. High Energy Phys. 1009 (2010) 091;
S. Chatrchyan, et al., CMS Collaboration, Phys. Lett. B 718 (2013);
G. Aad, et al., ATLAS Collaboration, Phys. Lett. B 725 (2013) 60;
ATLAS Collaboration, ATLAS-CONF-2015-027;
ATLAS Collaboration, ATLAS-COM-CONF-2015-033;
LHCb Collaboration, LHCb-CONF-2015-004;
LHCb Collaboration, CERN-LHCb-CONF-2015-004;
ALICE Collaboration, arXiv:1506.08032 [nucl-ex].
[16] K. Werner, B. Guiot, I. Karpenko, T. Pierog, in: Proceedings of 24th International Conference on Ultra-Relativistic Nucleus–Nucleus Collisions (Quark Matter 2014), Nucl. Phys. A 931 (2014) 83–91, arXiv:1411.1048 [nucl-th];
K. Dusling, R. Venugopalan, in: Proceedings of 24th International Conference on Ultra-Relativistic Nucleus–Nucleus Collisions (Quark Matter 2014), Nucl. Phys. A 931 (2014) 283;
I. Bautista, A.F. Tellez, P. Ghosh, arXiv:1505.00924 [hep-ph];
T. Altinoluk, N. Armesto, G. Beuf, A. Kovner, M. Lublinsky, arXiv:1503.07126 [hep-ph].
[17] B.I. Abelev, et al., STAR Collaboration, Phys. Rev. Lett. 97 (2006) 152301.
[18] K. Adcox, et al., PHENIX Collaboration, Phys. Rev. Lett. 88 (2002) 242301.
[19] B. Abelev, et al., STAR Collaboration, Phys. Lett. B 655 (2007) 104.
[20] B.B. Abelev, et al., ALICE Collaboration, Phys. Lett. B 736 (2014) 196.
[21] M. Aggarwal, et al., STAR Collaboration, Phys. Rev. C 83 (2011) 024901.
[22] B.B. Abelev, et al., ALICE Collaboration, Phys. Rev. Lett. 111 (2013) 222301.
[23] B. Abelev, et al., STAR Collaboration, Phys. Rev. C 75 (2007) 054906;
A. Adare, et al., PHENIX Collaboration, Phys. Rev. Lett. 98 (2007) 162301.
[24] R.C. Hwa, C.B. Yang, Phys. Rev. C 70 (2004) 024905;
R.J. Fries, B. Müller, C. Nonaka, S.A. Bass, Phys. Rev. C 68 (2003) 044902.
[25] A. Airapetian, et al., HERMES Collaboration, Nucl. Phys. B 780 (2007) 1;
A. Airapetian, et al., HERMES Collaboration, Eur. Phys. J. A 47 (2011) 113.
[26] G. Agakishiev, et al., STAR Collaboration, Phys. Rev. C 86 (2012) 064902.
[27] R.L. Ray, D.J. Prindle, T.A. Trainor, arXiv:1308.4367.
[28] B. Abelev, et al., STAR Collaboration, Phys. Rev. C 79 (2009) 034909.
[29] M. Anderson, et al., Nucl. Instrum. Methods Phys. Res., Sect. A, Accel. Spectrom. Detect. Assoc. Equip. 499 (2003) 659.
[30] R.J. Fries, Nucl. Phys. A 783 (2007) 125;
R.C. Hwa, arXiv:0904.2159 [nucl-th].
[31] M. Shao, et al., Nucl. Instrum. Methods Phys. Res., Sect. A, Accel. Spectrom. Detect. Assoc. Equip. 558 (2006) 419.
[32] J. Adams, et al., STAR Collaboration, arXiv:nucl-ex/0601042;
J. Adams, et al., STAR Collaboration, Phys. Lett. B 637 (2006) 161.
[33] B. Abelev, et al., Phys. Rev. C 77 (2008) 054901.
[34] S. Adler, et al., PHENIX Collaboration, Phys. Rev. C 71 (2005) 051902.
[35] K. Aamodt, et al., ALICE Collaboration, Phys. Rev. Lett. 108 (2012) 092301.
[36] L. Adamczyk, et al., STAR Collaboration, Phys. Rev. Lett. 112 (2014) 122301.
[37] S. Chatrchyan, et al., CMS Collaboration, Phys. Rev. C 90 (2014) 024908, arXiv: 1406.0932 [nucl-ex].
[38] G. Aad, et al., ATLAS Collaboration, Phys. Lett. B 739 (2014) 320, arXiv: 1406.2979 [hep-ex].

[39] S. Albino, B. Kniehl, G. Kramer, Nucl. Phys. B 725 (2005) 181.
[40] B. Mohanty, STAR Collaboration, in: Proceedings of the 23rd Winter Workshop on Nuclear Dynamics, 2007, arXiv:0705.0953.
[41] X.-N. Wang, Phys. Rev. C 58 (1998) 2321;
Q. Wang, X.-N. Wang, Phys. Rev. C 71 (2005) 014903;
S. Wicks, W. Horowitz, M. Djordjevic, M. Gyulassy, Nucl. Phys. A 784 (2007) 426;

N. Armesto, A. Dainese, C.A. Salgado, U.A. Wiedemann, Phys. Rev. D 71 (2005) 054027.
[42] J. Adams, et al., STAR Collaboration, Phys. Rev. C 72 (2005) 014904.
[43] K. Aamodt, et al., ALICE Collaboration, Phys. Lett. B 708 (2012) 249.
[44] B.B. Abelev, et al., ALICE Collaboration, arXiv:1405.4632 [nucl-ex].
[45] A. Adare, et al., PHENIX Collaboration, Phys. Rev. C 85 (2012) 064914.
[46] R. Lacey, J. Phys. G 38 (2011) 124048.